Large Eddy Simulation of a supersonic lifted flame using the Eulerian stochastic fields method

Yuri Paixão de Almeida[a], Salvador Navarro-Martinez[a,*]

[a]*Department of Mechanical Engineering, Imperial College London, Exhibition Road, South Kensington, London SW7 2AZ, UK*

Abstract

Scramjet propulsion systems can be the key to deliver the next generation of hypersonic planes. The high costs and complexity of gathering experimental data is a limiting factor in the development of such engine. In this context, numerical simulation has become increasingly popular to investigate supersonic combustion phenomena that otherwise would be prohibitively expensive. Despite recent progress, the simulation of high-speed compressible and reactive flows is still very challenging and presents many associated challenges. The chemical source term is highly non-linear and most combustion models are designed to operate in low-Mach number conditions. The present work investigates the use of Probability Density Function (PDF) in the context of Large Eddy Simulation models under supersonic conditions. Two approaches are considered: an extension of the joint scalar-enthalpy PDF for high-speed flows and a novel joint velocity-scalar-energy PDF model. Both formulations use the Eulerian stochastic fields approach implemented in a fully compressible density-based CFD code. The performance of the models

*Corresponding author:
Email address: s.navarro@imperial.ac.uk (Salvador Navarro-Martinez)

are investigated in a supersonic lifted flame, comparing the stochastic formulations with traditional models that neglect sub-grid fluctuations. The results show that sub-grid contributions are important at coarse meshes and the stochastic fields approach can reproduce the experimental data and the scatter observed. The simulations suggest that the scalar-enthalpy PDF is the most robust formulations and the sub-grid closures of the joint velocity-scalar PDF need further investigation.
Keywords:
Supersonic combustion, LES-PDF modelling, Eulerian stochastic fields, Lifted flame

---

1. Introduction

Supersonic combustion ramjets (scramjets) in air-breathing vehicle can achieve very high speeds (in excess of Mach 3 and even 5). However, characterisation of these systems is difficult. Experimental measurements of supersonic combustion systems are expensive and limited in scope. Computational Fluid Dynamics (CFD) techniques are often needed to complement the experimental data or offer new physical insights into the process.

Combustion at supersonic speeds presents strong interactions of the flow and the chemistry reactions. The high flow velocity reduces the residence time in the combustor, which leads to imperfect mixing of the reactants. This can cause instabilities, flame extinction and other finite-rate chemistry phenomena. This has several consequences for the modelling of supersonic combustion systems and creates additional challenges. The range of length

and time scales is wide and there is coupling between chemical time-scales and flow scales (Damköhler numbers are relatively low).

Large Eddy Simulations (LES) techniques have gained popularity in low-Mach combustion modelling. There is a wide range of *combustion modelling* techniques (see reviews [1, 2]) that have been applied with relative success. However, high-speed flows introduce constraints on the numerical solvers and combustion models employed. Supersonic flows are characterized by the presence of shocks that require specialised numerical techniques that often introduce numerical dissipation, destroying large-scale turbulence. Moreover, the high anisotropy of compressible flows reduces the validity of sub-grid modelling techniques. The number of unclosed terms in the filtered reactive Navier-Stokes equations also increase from 3 (assuming one reactive scalar) to 9.

The turbulent combustion modelling in LES focuses on closing the filtered reaction source term $\widetilde{S(\phi)}$. Combustion models in supersonic combustion have to capture finite-rate effects as well as the coupling between the velocity and energy/scalar fields. Conditional fluctuations of the reactive scalars (on a conserved scalar) are therefore likely to be larger than in subsonic combustion.

Nevertheless, conserved scalar models have been used for supersonic combustion LES [3, 4] due to their low computational cost. Most of the recent examples of LES of supersonic combustion [5–7] assume quasi-laminar (QL) combustion $\widetilde{S} \sim S\left(\widetilde{\phi}\right)$ which implies that scalars below the filter width are perfectly mixed (homogeneous reactor). The Partially Stirred Reactor (PaSR) model includes the effects of sub-grid fluctuations through a fine-scale

structures function [8]. Similarly, the extension U-PaSR model has also been applied to supersonic combustion [9]. Alternatively, the transported probability density (PDF) approach can be used. The PDF approach accounts for all (or some) of the sub-grid non-homogeneities. Two major resolution methods for the PDF equation exist in the supersonic context. The DQMOM approach, which resolves only a few moments of the sub-grid PDF [10, 11]; and stochastic Monte Carlo techniques [12].

It is clear that if very fine meshes are used, the sub-grid contributions will become small and errors using the QL approach would be minor, especially if time-averaged statistics are considered. For instance, Bouheraoua et al. [7] finest grid was $\sim 5\eta_k$, where η_k is the estimated Kolmogorov scale. If the filter width is close to Kolmogorov scales, QL approaches will produce good results, at least in non-premixed combustion, as the cell can be considered well-stirred and quasi-homogeneous reactors [13]. However, the associated costs of computing such meshes can be very large, especially modelling full combustors or using detailed chemistry (doubling the number of grid points in each direction, increases the cost by sixteen times). PDF methods can have a better accuracy-cost ratio at intermediate meshes as they can account for sub-grid homogeneities and reduce the number of unclosed terms. The objective of this work is to investigate the performance of stochastic PDF approaches in a supersonic turbulent flame. Two Eulerian LES-PDF approaches are implemented, a joint scalar-enthalpy PDF and a novel joint velocity-scalar-energy formulation. Both methods use the Eulerian stochastic fields technique; which has only been applied once to supersonic combustion [12]. - The simulation results are therefore compared to QL models at the

same resolution.

2. The LES-PDF approach for compressible flows

PDF methods [14] have been used to overcome the modelling requirement for the reactive source term and the convective closure on RANS and LES approaches.

Most LES-PDF methods have been developed using the low-Mach number assumption. In this hypothesis a reference pressure is used on the reactive term, making it a function of thermo-chemical variables, such as enthalpy and species mass fraction. Under this hypothesis, a LES-PDF model can be developed including only species mass fraction and enthalpy on its sample space and it is able to solve exactly the chemical source term [14].

In reactive compressible flows, another thermodynamic variable has to be included to close the source term. Common choices are: pressure [15, 16] or density [17]. It is also possible to include the velocity components in the sample space to close the convective part [15, 16], also a relevant term on high-speed flows.

Here two novel LES-PDF approaches are proposed to simulate high-speed reactive flows. The first is a scalar LES-PDF (SPDF) inspired by Gerlinger [18] work, however, using the Eulerian stochastic fields technique [19, 20] to solve the LES-PDF equation. The second is a new velocity-scalar LES-PDF (VSPDF), in which the velocity and density are also included into the PDF sample space, similarly to [17, 21], also using the stochastic fields.

2.1. Scalar LES-PDF

In this method the enthalpy and mass fractions variables are included into the sample space of the fine-grained Eulerian PDF:

$$f'(\eta, Z_\alpha; \boldsymbol{x}, t) = \delta(h(\boldsymbol{x}, t) - \eta)\delta(Y_\alpha(\boldsymbol{x}, t) - Z_\alpha) \tag{1}$$

where η, Z_α are the sample (or phase) enthalpy and mass fractions; and $h(\boldsymbol{x}, t)$ and $Y_\alpha(\boldsymbol{x}, t)$ are the "real" enthalpy and mass fractions, respectively. The LES-PDF equation therefore can be obtained by deriving a transport equation for f' and applying a spatial filter [22]. In this work the (IEM) micromixing model [23] is employed to close remaining viscous terms. The closed LES-PDF equation is:

$$\begin{aligned}
&\frac{\partial \overline{\rho}\widetilde{f}}{\partial t} + \frac{\partial \overline{\rho}\widetilde{u}_i\widetilde{f}}{\partial x_i} = \frac{\partial}{\partial x_i}\left(\Gamma' \frac{\partial \widetilde{f}}{\partial x_i}\right) \\
&- \frac{\partial}{\partial Z_\alpha}\left(\overline{\rho} S_\alpha\left(\overline{p}, \boldsymbol{\Psi}\right)\widetilde{f} - \frac{1}{2}\frac{C_{Y_\alpha}}{\tau_{sgs}}\overline{\rho}\left(Z_\alpha - \widetilde{Y}_\alpha\right)\widetilde{f}\right) \\
&- \frac{\partial}{\partial \eta}\left(\frac{D\overline{p}}{Dt}\widetilde{f} + \widetilde{\tau}_{ij}\frac{\partial \widetilde{u}_i}{\partial x_j}\widetilde{f} - \frac{1}{2}\frac{C_H}{\tau_{sgs}}\overline{\rho}\left(\eta - \widetilde{h}\right)\widetilde{f}\right)
\end{aligned} \tag{2}$$

where $\Gamma' = \mu/\sigma + \mu_{sgs}/\sigma_{sgs}$ is the total diffusion coefficient and $\tau_{sgs} = \left(\mu + \mu_{sgs}/\overline{\rho}\Delta^2\right)^{-1}$ [24]. The Schmidt number σ and its sub-grid equivalent σ_{sgs} are equal to unity, like the Prandtl numbers, for simplicity. The sub-grid mixing constants C_{Y_α} and C_H are equal to 2. The proposed LES-PDF equation relies on the assumption that the reactive source term is a function of sample variables and the filtered pressure. The source term is therefore partially modelled as $\widetilde{S}_\alpha \approx S_\alpha\left(\overline{p}, \boldsymbol{\Psi}\right)$, where $\boldsymbol{\Psi} = [\eta, Z_\alpha]$.

This assumption has been applied by several authors [12, 18, 25, 26] in order to avoid the inclusion of one more thermodynamic variable into the

LES-PDF equation. The pressure used to close the source term is not a reference pressure though, but the same local pressure that is used within the compressible flow solver. However, as pointed out by Gerlinger [18], there has not been any investigation to evaluate the magnitude of possible errors resulting from this assumption.

Eulerian stochastic differential equations for the mass fractions and enthalpy are then obtained using the same method as [20]. The equations for the n$^{\text{th}}$-set of Eulerian stochastic fields are:

$$\begin{aligned}\overline{\rho}\frac{d\mathscr{Y}_\alpha^n}{dt}+\overline{\rho}\widetilde{u}_i\frac{\partial\mathscr{Y}_\alpha^n}{\partial x_i}=\frac{\partial}{\partial x_i}\left(\Gamma'\frac{\partial\mathscr{Y}_\alpha^n}{\partial x_i}\right)+\overline{\rho}S_\alpha^n\left(\overline{p},\mathbf{\Psi}\right)\\-\frac{1}{2}\frac{C_{Y_\alpha}}{\tau_{sgs}}\overline{\rho}\left(\mathscr{Y}_\alpha^n-\widetilde{Y}_\alpha\right)+\left(2\overline{\rho}\Gamma'\right)^{1/2}\frac{\partial\mathscr{Y}_\alpha^n}{\partial x_i}\frac{\mathrm{d}W_i^n}{\mathrm{d}t}\end{aligned}\tag{3}$$

$$\begin{aligned}\overline{\rho}\frac{d\mathscr{H}^n}{dt}+\overline{\rho}\widetilde{u}_i\frac{\partial\mathscr{H}^n}{\partial x_i}=\frac{\partial}{\partial x_i}\left(\Gamma'\frac{\partial\mathscr{H}^n}{\partial x_i}\right)+\frac{D\overline{p}}{Dt}+\widetilde{\tau}_{ij}\frac{\partial\widetilde{u}_i}{\partial x_j}\\-\frac{1}{2}\frac{C_H}{\tau_{sgs}}\overline{\rho}\left(\mathscr{H}^n-\widetilde{h}\right)+\left(2\overline{\rho}\Gamma'\right)^{1/2}\frac{\partial\mathscr{H}^n}{\partial x_i}\frac{\mathrm{d}W_i^n}{\mathrm{d}t}\end{aligned}\tag{4}$$

where $\mathscr{Y}_\alpha^n$ and $\mathscr{H}^n$ are the stochastic fields for mass fractions and enthalpy, respectively. The Wiener process dW_i^n is approximated by $dt^{1/2}\gamma$, where $\gamma=\{-1,1\}$ is a dichotomic vector [19], ensuring that $\langle dW_i\rangle=0$, where $\langle\cdot\rangle$ denotes arithmetic mean. Filtered quantities are calculated from the average of the stochastic fields as $\widetilde{Q}\approx\langle Q\rangle$.

The novelty of this model is the closure of the filtered pressure without neglecting any subgrid terms, as usually performed in LES simulations. The filtered pressure field is obtained using the ideal gas law as:

$$\overline{p}=\overline{\rho}\widetilde{RT}\approx\overline{\rho}R_u\left[\frac{1}{N_F}\sum_{n=1}^{N_F}\left(\sum_{\alpha=1}^{N_s}\frac{\mathscr{Y}_\alpha^n}{W_\alpha}\right)T^n\right]\tag{5}$$

where R_u is the gas universal constant, W_α is the molecular weight of the chemical specie α and N_F is the number of stochastic fields.

The Eulerian stochastic fields equations are coupled with a traditional LES compressible solver to calculate the remaining variables such as filtered density and velocity. The total energy equation, although redundant, is also solved in order to increase numerical stability. The sub-grid stresses are closed using a conventional Smagorinsky model to evaluate the sub-grid viscosity μ_{sgs}.

2.2. Velocity-scalar LES-PDF

On this novel formulation we include in the sample space the velocity and density, along with the total energy instead of enthalpy. The fine-grained Eulerian PDF is defined as the following:

$$\begin{aligned} f'(d, v_i, \zeta, Z_\alpha; \boldsymbol{x}, t) =& \delta(\rho(\boldsymbol{x}, t) - d)\delta(u_i(\boldsymbol{x}, t) - v_i)\times \\ & \delta(e_t(\boldsymbol{x}, t) - \zeta)\delta(Y_\alpha(\boldsymbol{x}, t) - Z_\alpha) \end{aligned} \tag{6}$$

where d, v_i, ζ and Z_α are the sample density, velocity, total energy and mass fraction. It is possible again to obtain a LES-PDF equation by deriving a transport equation for f' and applying the spatial filtering operation:

$$\begin{aligned} & \frac{\partial \overline{\rho}\widetilde{f}}{\partial t} + \frac{\partial \overline{\rho} v_i \widetilde{f}}{\partial x_i} = -\frac{\partial}{\partial d}\left(-\overline{\rho}^2 \frac{\partial \widetilde{u_i}}{\partial x_i}\widetilde{f}\right) \\ & - \frac{\partial}{\partial Z_\alpha}\left(\frac{\partial \widetilde{J}_{\alpha,i}}{\partial x_i}\widetilde{f} + \overline{\rho} S_\alpha\left(\boldsymbol{\Phi}\right)\widetilde{f} - \frac{1}{2} C_{Y_\alpha}\frac{\epsilon}{k}\overline{\rho}\left(Z_\alpha - \widetilde{Y_\alpha}\right)\widetilde{f}\right) \\ & - \frac{\partial}{\partial v_i}\left(-\frac{\partial \overline{p}}{\partial x_i}\widetilde{f} + \frac{\partial \widetilde{\tau}_{ij}}{\partial x_i}\widetilde{f} + \overline{\rho} G_{ij}\left(v_j - \widetilde{u}_j\right)\widetilde{f}\right) \\ & + \frac{\partial^2}{\partial v_i \partial v_i}\left(\frac{1}{2} C_0 \epsilon \widetilde{f}\right) \\ & - \frac{\partial}{\partial \zeta}\left(\frac{\partial \widetilde{q}_i}{\partial x_i}\widetilde{f} - \frac{\partial \overline{p}\widetilde{u}_i}{\partial x_i}\widetilde{f} + \frac{\partial \widetilde{\tau}_{ij}\widetilde{u}_j}{\partial x_i}\widetilde{f} - \frac{1}{2} C_{e_t}\frac{\epsilon}{k}\overline{\rho}\left(\zeta - \widetilde{e_t}\right)\widetilde{f}\right) \end{aligned} \tag{7}$$

where k and ϵ are the sub-grid kinetic energy and its dissipation, respectively. They are modelled here using the same model as Nik *et al.* Nik et al. [16]. Equation (7) is written in closed form, where the micromixing IEM [23] and the simplified Langevin model [14] are used to close the remaining unknowns. In the simplified Langevin framework, the tensor is defined as $G_{ij} = -(1/2 + 3/4C_0)(\epsilon/k)\delta_{ij}$ with $C_0 = 2.1$.

In this formulation the convective terms and the source $S_\alpha(\mathbf{\Phi})$, $\mathbf{\Phi} = [d, v_i, \zeta, Z_\alpha]$, are exactly closed. The proposed new n^{th}-set of Eulerian stochastic fields equations is:

$$\frac{d\varrho^n}{dt} + \frac{\partial \varrho^n \mathscr{U}_i^n}{\partial x_i} = 0 \tag{8}$$

$$\begin{aligned}\varrho^n \frac{d\mathscr{U}_i^n}{dt} + \varrho^n \mathscr{U}_j^n \frac{\partial \mathscr{U}_i^n}{\partial x_j} &= -\frac{\partial \mathscr{P}^n}{\partial x_i} + \frac{\varrho^n}{\overline{\rho}} \frac{\partial \widetilde{\tau}_{ij}}{\partial x_i} \\ &+ \varrho^n G_{ij}\left(\mathscr{U}_j^n - \widetilde{U}_j\right) + \varrho^n \left(C_0 \frac{\epsilon}{\overline{\rho}}\right)^{1/2} \frac{\mathrm{d}W_i^n}{\mathrm{d}t}\end{aligned} \tag{9}$$

$$\begin{aligned}\varrho^n \frac{d\mathscr{Y}_\alpha^n}{dt} + \varrho^n \mathscr{U}_i^n \frac{\partial \mathscr{Y}_\alpha^n}{\partial x_i} &= \frac{\varrho^n}{\overline{\rho}} \frac{\partial \widetilde{J}_{\alpha,i}}{\partial x_i} + \varrho^n S_\alpha^n(\mathbf{\Phi}) \\ &- \frac{1}{2} C_{Y_\alpha} \frac{\epsilon}{k} \varrho \left(\mathscr{Y}_\alpha^n - \widetilde{Y}_\alpha\right)\end{aligned} \tag{10}$$

$$\begin{aligned}\varrho^n \frac{d\mathscr{E}_t^n}{dt} + \varrho^n \mathscr{U}_i^n \frac{\partial \mathscr{E}_t^n}{\partial x_i} &= \frac{\varrho^n}{\overline{\rho}} \frac{\partial \widetilde{q}_i}{\partial x_i} - \frac{\varrho^n}{\overline{\rho}} \frac{\partial \overline{p}\widetilde{u}_i}{\partial x_i} + \\ &\frac{\varrho^n}{\overline{\rho}} \frac{\partial \widetilde{\tau}_{ij}\widetilde{u}_j}{\partial x_i} - \frac{1}{2} C_{e_t} \frac{\epsilon}{k} \varrho \left(\mathscr{E}_t^n - \widetilde{e}_t\right)\end{aligned} \tag{11}$$

where ϱ^n, $\mathscr{U}_i^n$, $\mathscr{Y}_\alpha^n$ and $\mathscr{E}_t^n$ are the stochastic fields for density, velocity, mass fraction and total energy. These equations are obtained using similar techniques as Soulard and Sabel'nikov [27]. Sub-grid compressible effects caused by pressure-dilatation and dilatation-dissipation correlations have been neglected in this work, but could be included within the Langevin model [15].

Every set of stochastic differential equations obeys its own continuity equation, respecting field-mass balance. Also, each set has its own stochastic pressure field, $\mathscr{P}^n$, which is obtained from the stochastic variables as $\mathscr{P}^n = \mathscr{P}^n\left(\varrho^n, \mathscr{Y}_\alpha^n, \mathscr{E}_t^n\right)$. The use of the stochastic pressure guarantees the stability of the solution of each individual field compared to the use of filtered pressure $\overline{p}$. However, the formulation requires closure of the sub-grid compressibility effects [15]. This contribution has been neglected in the present LES-VSPDF. This could cause artificial damping on pressure fluctuations.

If the filtered pressure is used, the solution for the system of SPDE hyperbolic equations equivalent to (7) could be multivalued [28], which cannot be described by single-point PDF and could lead to stochastic sub-grid shocks. In this model, filtered quantities are then obtained from the fields average $\overline{Q} \approx \langle Q \rangle$ and Favre filtered quantities from the density-weighted average $\widetilde{Q} \approx \langle \varrho Q \rangle / \langle \varrho \rangle$.

3. Methodology

3.1. Test Case

The models developed in the previous section are evaluated through the simulation of the benchmark case of Cheng et al. [29]. This test case has been widely used on validation of supersonic combustion models [6, 7, 9, 30]. It consist of a co-flowing axi-symmetric supersonic jet hydrogen diffusion flame. The configuration of the burner is described in Table 1. The fuel injection is sonic and the resultant flow field was observed to be highly unstable in the experiments Cheng et al. [29].

The operational Reynolds number at the exit of the fuel injector is 15600

Table 1: Supersonic burner configuration [29]

Dimensions	
Nozzle exit inner diameter	17.78 mm
Fuel injector inner diameter	2.36 mm
Fuel injector outer diameter	3.81 mm
Vitiated air exit conditions	
Pressure	107 kPa
Temperature	1250 K
Mach number	2.0
Velocity	1420 m/s
O_2 mole fraction	0.201
N_2 mole fraction	0.544
H_2O mole fraction	0.255
Fuel exit conditions	
Pressure	112 kPa
Temperature	540 K
Mach number	1.0
Velocity	1780 m/s
H_2 mole fraction	1.0

and on the vitiated air injector is 101100. This burner generates a lifted-flame, which results in a very intermittent behaviour with several auto-ignition and partial-extinction cycles. The Kolmogorov length and time scales range from 8-35 μm, with integral scales between 3 and 7 mm and from 0.2-14.2 μs [29]. The estimated Damköhler number are of $\mathcal{O}(1)$ close

to the flame base.

3.2. Numerical modelling

The stochastic equations are implemented into the compressible in-house finite difference code CompReal. Spatial discretisation of the convective terms is performed using a hybrid 11-2 DRP (Dispersion-Relation-Preserving) scheme [31] and HLLC (Harten-Lax-van Leer-Contact) Riemann-Solver [32]. Both schemes are coupled through the use of a sensor based on large density and scalar gradients. A fourth-order central difference scheme is applied for the viscous terms and remaining derivatives. The explicit first order Euler-Maruyama temporal discretisation [33] is employed to solve the stochastic partial differential equations. In the SPDF model, the filtered equations for density, velocity and total energy are solved with an explicit third-order Runge-Kutta temporal scheme.

A domain of size of 70D $\times$ 60D $\times$ 60D is chosen, where D is the fuel injector inner diameter. Two Cartesian grids are employed with stretching close to the centreline following [7], increasing the number of elements in the flame region. Two grids are used, a coarse mesh with 200000 elements and a second one with approximately 2 million (2M). In the inlet, supersonic Dirichlet conditions are applied, On the fuel and vitiated air injection the specified conditions in Table 1 are used; while a synthetic turbulence of 5% of the axial velocity is added on the vitiated air injection only through the use of a digital filter. A zero gradient conditions on the lateral sides and outflow boundary is used.

The advantage of the PDF methods is their ability to solve with greater accuracy the chemical source term, allowing the use of complex chemistry

mechanism. The CHEMKIN package is used here to calculate the chemical source term using an implicit ODE solver. The skeletal mechanism of Yetter et al. [34] is used to describe the combustion of hydrogen. This mechanism uses 9 chemical species and 19 reactions.

The simulations evaluated four different LES models. These models are the implicit LES (ILES), Smagorinsky LES, SPDF and VSPDF. The ILES contains no modelling to describe the convective part or source term. The Smagorinsky LES is the classical large eddy simulation model to close the convective terms only, with the QL approach for the source term. The SPDF and VSPDF are simulated with 8 stochastic fields. A simulation with 16 fields for the VSPDF was also performed, but it did not show significant difference from the 8 fields simulation. The simulations run for approximately 2 ms [7] after the flow stabilises, sufficient to extract temporal averaged results.

The computational cost associated to the Eulerian stochastic fields can be estimated by the number of fields times the required cost to run a single field. Therefore, the cost of the 8 fields simulation is approximately eight times the simulation with one field in the same mesh (also the cost of ILES). The Smagorinsky LES is marginally more expensive than ILES. To assess the cost-performance of the model, the coarse mesh LES-PDF simulations would have to be more accurate than the Smagorinsky model with a refined mesh.

4. Results

Figure 1 presents an overall picture of the results obtained. It shows average temperatures and OH molar fraction distribution at the centreline of

the flame. The SPDF model produces the best agreement with experimental temperature. Figure 1 illustrates that the Smagorinsky model, even with the finer mesh, cannot reproduce the experimental data as well as the SPDF model.

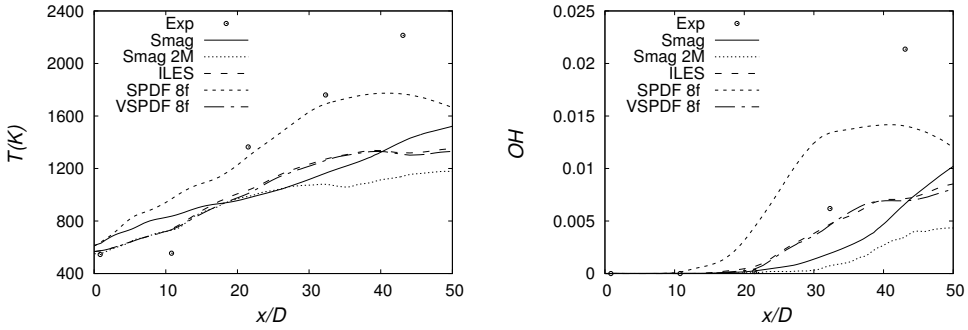

(a) (b)

Figure 1: (a) and (b): Mean temperature and OH molar fraction centreline profiles, respectively.

The VSPDF performs (in average) similarly to ILES, predicting lower temperatures. The present VSPDF formulation predicts lower fluctuations (even if sub-grid velocity fluctuations of 30% are recorded). This could be attributed to the sensitivity to turbulent dissipation modelling or the difficulty of implementing sub-grid boundary conditions for velocity. The inlet boundary conditions for the VSPDF model do not have sub-grid contributions (i.e. the incoming PDF is a Dirac PDF). The inlet velocity boundary condition is the same for all fields, neglecting sub-grid fluctuations. This is the same as the ILES model and indeed the behaviour of both models is the same close to the injector. This could explain why the VSPDF model shows lower fluctuations than SPDF, as the VSPDF needs to generate sub-

grid fluctuations first, before scalar fluctuations are generated. Similarly, the neglected sub-grid pressure-dilatation and compressibility correlations may play a bigger role than expected.

Temperature values close to the burner are quite higher for the SPDF and for the Smagorinsky (coarse mesh). This could be explained by the increased viscous effects due to the turbulent viscosity model. As the grid is refined, this effect diminishes and it can be seen by the similarity between the refined Smagorinsky (2M) and the ILES and VSPDF models performance.

The OH distribution, as shown in Fig. 1, can represent the flame position. While for the SPDF the flame base is relatively well defined, with high OH concentration, the remaining models show slower development of this radical. The SPDF over-predicts OH until $x/D = 32.3$, where it starts decaying. The experimental lift-off height is approximately 25 D. The lift-off height (based on the maximum OH gradient) for the SPDF is 26.25 D; 32.37 (VSPDF) and 26.72 (ILES); while Smagorinsky is around 38 jet diameters.

Experimental data for scatter plots is also provided and shown here. The standard deviation of the single-shot can be up to 13.2% for the OH and 11.7% for the temperature with smaller numbers for H_2 and H_2O. Figures 2 and 3 shows scatter plots of OH molar fraction at $x/D = 43.1$. The mixture fraction f used is the same defined by Boivin et al. [6]. While the VSPDF and Smagorinsky simulation shows data close to the equilibrium line, the SPDF model show a similar scatter to the experimental data, with many super-equilibrium points. The Smagorinsky results model are similar to Boivin et al. [35], although they show less scatter; probably due to the coarse mesh employed.

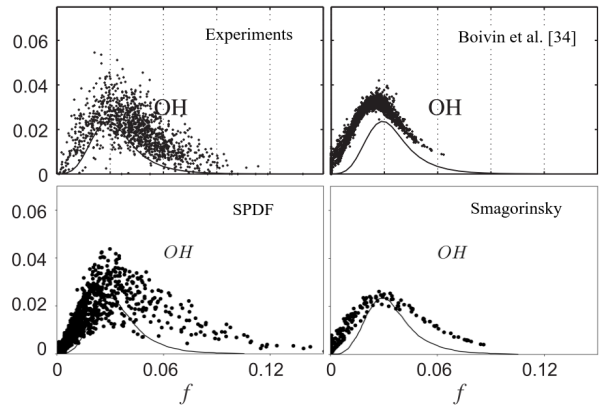

Figure 2: Scatter of OH molar fraction at position x/D=43.1 and t = 2ms, showing experimental data Cheng et al. [29] (upper left), results from Boivin et al. [35] (upper right) and present Scalar-PDF (lower left) and Smagorinsky results with the coarse mesh (lower right). The solid represent the adiabatic equilibrium line.

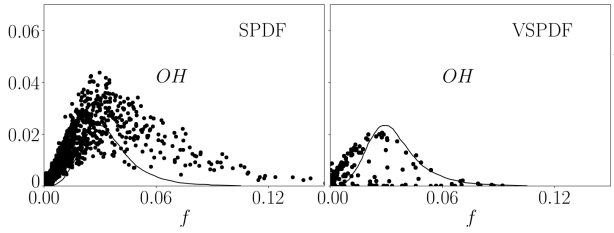

Figure 3: Scatter of OH molar fraction at position x/D=43.1 and t = 2ms, showing the present Scalar PDF (left) and the velocity-scalar PDF (right). The solid represent the adiabatic equilibrium line.

Figure 4 shows scatter plots of H_2O and O_2 molar fraction at $x/D = 43.1$ and t=2ms. For the SPDF and Smagorinsky models, the scattering follows more closely the equilibrium line, while the SPDF presents a wider range of values and better agreement with experimental data. The VSPDF shows points close to both equilibrium and mixing without reaction lines, indicating that combustion is not fully developed yet.

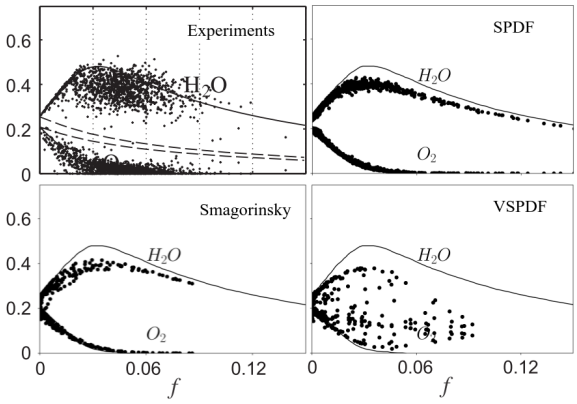

Figure 4: Scatter of H_2O and O_2 molar fraction at position x/D=43.1 and t = 2ms, showing experimental data Cheng et al. [29] (upper left), the present Scalar PDF (upper right), Smagorinsky with coarse mesh (lower left) and Velocity-Scalar PDF (lower right). The solid represent the adiabatic equilibrium line.

Scatter plots of temperature are presented in Fig. 5 for the SPDF model at two different positions, $x/D = 32.3$ and 43.1. Overall, there is a qualitative reasonable agreement with the experimental data, with the numerical results presenting higher concentration of spots with small mixture fraction value and temperature.

The scatter plots suggest that the flame has a very unstable behaviour. Figure 6 shows the OH molar fraction using the VSPDF model. The flame is relatively narrow. This could be attributed by the relatively "poor" mixing of the VSPDF model. The SPDF model, automatically increases sub-grid mixing in regions of high scalar gradients, while the VSPDF does so indirectly through the sub-grid velocity fluctuations. See the small scatter of SPDF in Figures 3 and 5. In the present flame, higher sub-grid mixing in turn increase the overall heat release rate. With the VSPDF model, The reaction spots are barely connected and the flame resembles a low Mach number

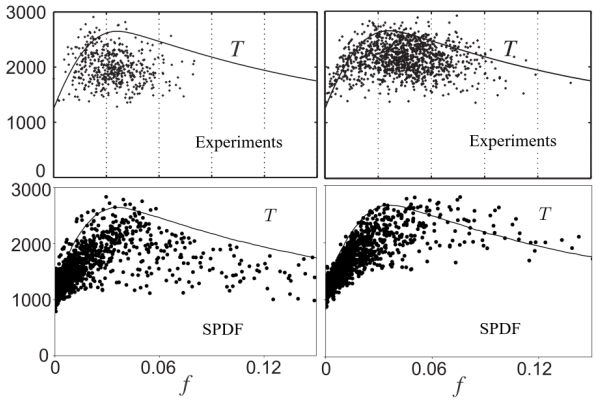

Figure 5: Experimental data at positions x/D=32.3 (upper left) and x/D=43.1 (upper right) from Cheng et al. [29], along with its adiabatic equilibrium line. Image from Boivin et al. [35]. Results for SPDF 8 fields simulation with coarse mesh at positions x/D=32.3 (lower left) and x/D=43.1 (lower right) at t = 2ms.

auto-ignition flame [36]. Overall, even with fine meshes, the SPDF still outperforms Smagorinsky model (see Fig. 7).

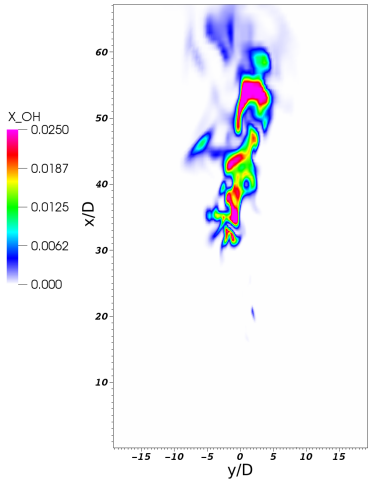

Figure 6: Contour plot of instantaneous OH molar fraction, VSPDF simulation with 2M points. Time step at 0.96 ms.

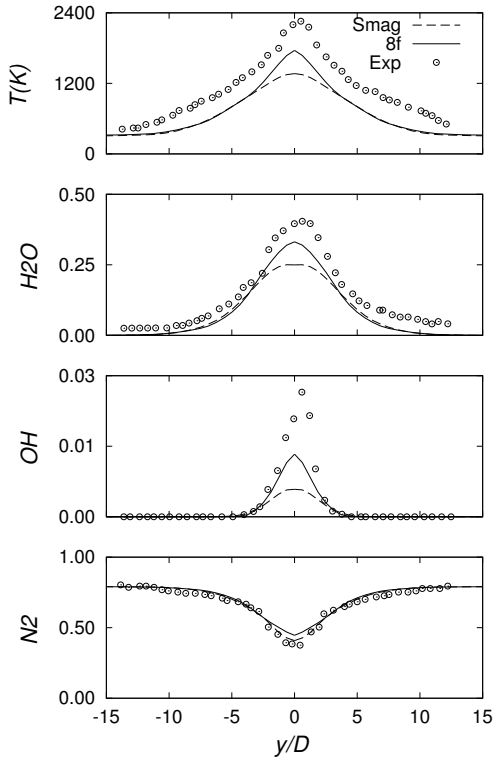

Figure 7: Radial distribution of SPDF and Smagorinsky model at $x/D = 43.1$.

5. Conclusions

Simulations of the supersonic burner of Cheng et al. [29] have been performed employing several LES models. Two LES-PDF formulations are evaluated along with the QL combustion model with Smagorinsky LES and ILES framework. The novel scalar-PDF approach has the best performance even with a coarse mesh in comparison to the QL/Smagorinsky model. The results for the SPDF are within the same order of magnitude of experimental data and are cheaper than comparable results with the QL/Smagorinsky approach at much finer meshes. Overall the agreement of the SPDF model

with experimental data is satisfactory, and the model is able to capture the flame behaviour. The SPDF model is a promising tool for complex chemistry simulations at high-speed flows, allowing quantitative estimation of the OH radical, and therefore provide insight into the flame structure. The similar VSPDF proposed model, underestimates the sub-grid fluctuations suggesting that the pressure-correlation terms or the sub-grid boundary conditions need further closures.

Acknowledgments

Yuri P. Almeida acknowledges the financial support provided by the Brazilian National Council for Scientific and technological Development (CNPq) through the Science without Borders programme, grant no. 233815/2014-7.

References

[1] H. Pitsch, Annu. Rev. Fluid Mech. 38 (2006) 453–482.

[2] C. Fureby, Phil. Trans. A 367 (2009) 2957–69.

[3] M. Berglund, C. Fureby, Proc. Combust. Inst. 31 (2007) 2497–2504.

[4] V. E. Terrapon, F. Ham, R. Pecnik, H. Pitsch, A flamelet-based model for supersonic combustion, Technical Report, Center for Turbulence Research, 2009.

[5] J. R. Edwards, J. A. Boles, R. A. Baurle, Combust. Flame 159 (2012) 1127–1138.

[6] P. Boivin, A. Dauptain, C. Jiménez, B. Cuenot, Combust. Flame 159 (2012) 1779–1790.

[7] L. Bouheraoua, P. Domingo, G. Ribert, Combust. Flame 179 (2017) 199–218.

[8] C. Fureby, M. Chapuis, E. Fedina, S. Karl, Proc. Combust. Inst. 33 (2011) 2399–2405.

[9] Y. Moule, V. Sabelnikov, A. Mura, Combust. Flame 161 (2014) 2647–2668.

[10] P. Donde, H. Koo, V. Raman, J. Comput. Phys. 231 (2012) 5805–5821.

[11] H. Koo, P. Donde, V. Raman, Proc. Combust. Inst. 33 (2011) 2203–2210.

[12] C. Gong, M. Jandi, X. Bai, J. Liang, M. Sun, International Journal of Hydrogen Energy 42 (2017) 1264–1275.

[13] C. Duwig, K. Nogenmyr, C. Chan, M. J. Dunn, Combustion Theory and Modelling 15 (2011) 537–568.

[14] S. B. Pope, Progress in Energy and Combustion Science 11 (1985) 119–192.

[15] B. J. Delarue, S. B. Pope, Physics of Fluids 9 (1997) 2704–2715.

[16] M. B. Nik, P. Givi, C. K. Madnia, S. B. Pope, in: 50th AIAA Aerospace Sciences Meeting including the New Horizons Forum and Aerospace Exposition, Tennessee, 2012.

[17] J. Bakosi, J. R. Ristorcelli, Journal of Turbulence 11 (2010).

[18] P. Gerlinger, Journal of Computational Physics 339 (2017) 68–95.

[19] L. Valiño, Flow, Turbulence and Combustion 60 (1998) 157–172.

[20] V. Sabel'nikov, O. Soulard, Physical Review E 72 (2005) 1282–1284.

[21] P. Eifler, W. Kollmann, in: 31st Aerospace Sciences Meeting & Exhibit, Reno, 1993.

[22] D. C. Haworth, Progress in Energy and Combustion Science 36 (2010) 168–259.

[23] J. Villermaux, J. C. Devillon, in: 2nd International Symposium on Chemical Reaction Engineering, Netherlands, 1972.

[24] W. P. Jones, S. Navarro-Martinez, Combust. Flame 150 (2007) 170–187.

[25] H. Möbus, P. Gerlinger, D. Brüggemann, Combustion and Flame 132 (2003) 3–24.

[26] A. Banaeizadeh, Z. Li, F. A. Jaberi, AIAA Journal 49 (2011) 2130–2143.

[27] O. Soulard, V. A. Sabel'nikov, Combustion, Explosion and Shock Waves 42 (2006) 753–762.

[28] N. Petrova, Turbulence-chemistry interaction models for numerical simulation of aeronautical propulsion systems, Ph.D. thesis, Ecole Polytechnique, Paris, 2015.

[29] T. S. Cheng, J. A. Wehrmeyer, R. W. Pitz, O. Jarrett Jr, G. B. Northam, Combust. Flame 99 (1994) 157–173.

[30] A. Dauptain, B. Cuenot, T. J. Poinsot, in: Complex Effects in Large Eddy Simulation, Limassol, 2005.

[31] C. K. W. Tam, J. C. Webb, J. Comput. Phys. 107 (1993) 262–281.

[32] E. F. Toro, M. Spruce, W. Speares, Shock Waves 4 (1994) 25–34.

[33] P. E. Kloeden, E. Platen, Numerical Solution of Stochastic Differential Equations, Springer, Berlin, 1st edition, 1992.

[34] R. A. Yetter, F. L. Dryer, H. Rabitz, Combustion Science and Technology 79 (1991) 97–128.

[35] P. Boivin, A. Dauptain, C. Jiménez, B. Cuenot, Combustion and Flame 159 (2012) 1779–1790.

[36] W. P. Jones, S. Navarro-Martinez, Comp. & Fuids 37 (2008) 802–808.